

On the Electronic Structure of Neutral and Ionic Azobenzenes and Their Possible Role as Surface Mounted Molecular Switches

Gernot Fuchs, Tillmann Klamroth, Jadranka Dokić, and Peter Saalfrank*

Theoretische Chemie, Institut für Chemie, Universität Potsdam, Karl-Liebknecht-Straße 24-25,
D-14476 Potsdam-Golm, Germany

Received: February 15, 2006; In Final Form: June 1, 2006

We report quantum chemical calculations, mostly based on density functional theory, on azobenzene and substituted azobenzenes as neutral molecules or ions, in ground and excited states. Both the cis and trans configurations are computed as well as the activation energies to transform one isomer into the other and the possible reaction paths and reaction surfaces along the torsion and inversion modes. All calculations are done for the isolated species, but results are discussed in light of recent experiments aiming at the switching of surface mounted azobenzenes by scanning tunneling microscopes.

1. Introduction

Azobenzene dyes have been extensively studied recently, both theoretically^{1–11} and by experiment,^{4,12–22} because of their ability to undergo reversible cis–trans isomerization upon optical excitation. This makes them promising candidates for digital storage devices, or molecular switches.²³

It has been shown very recently that azobenzenes can also be manipulated with a scanning tunneling microscope (STM) tip when adsorbed on a (gold) surface. The manipulations that were achieved are rotation or translation of the molecules,²⁴ or, more interestingly, their cis–trans isomerization.^{13,25,26} There are various mechanisms by which an STM can enforce reactions: (i) by “above threshold excitation” of an adsorbate with single electrons or holes, (ii) by inelastic electron tunneling (IET) with more than one charge carrier, or (iii) by field effects. The first two are resonant, resulting in reaction yields that depend linearly or nonlinearly on the tunneling current, respectively, while the latter is operative even in the zero-current limit. In comparison to photons, the STM thus not only offers a molecular resolution and thus a maximal storage capacity in possible applications, but also, new reaction pathways and intermediate states become accessible. In the resonant cases, for example, negative and positive ion states are used as intermediates depending on whether the bias voltage is positive or negative.

Specifically, for the present work, the following experimental observations are interesting. In ref 13, evidence for reversible cis–trans isomerization of the azobenzene derivative disperse orange 3 $\text{H}_2\text{N}-\text{C}_6\text{H}_4-\text{N}=\text{N}-\text{C}_6\text{H}_4-\text{NO}_2$ (henceforth DO3) on Au(111) by IET at positive bias voltages of about 650 meV and larger has been given. In ref 26, dimetacyano-azobenzene $\text{NC}-\text{C}_6\text{H}_4-\text{N}=\text{N}-\text{C}_6\text{H}_4-\text{CN}$ (henceforth DMC) and 2,13-carboxymethylester-azobenzene (CMA) $\text{H}_3\text{C}-\text{COO}-\text{C}_6\text{H}_4-\text{N}=\text{N}-\text{C}_6\text{H}_4-\text{COOCH}_3$ molecules on the same surface were either desorbed or switched probably from trans to either cis or a rotated form. The reaction occurred at positive voltages of about 1.6 and 2.3 V, respectively, for DMC and CMA. And finally, on gold surfaces, tetra-*tert*-butyl-azobenzene $(\text{H}_3\text{C})_3\text{C}-\text{C}_6\text{H}_3-\text{N}=\text{N}-\text{C}_6\text{H}_3(\text{C}(\text{CH}_3)_3)_2$ (henceforth TTA) was switched, probably from cis to trans and vice versa.²⁵ Interestingly, the switching occurs both at positive and at negative sample bias here, and even in the zero-current limit.²⁵

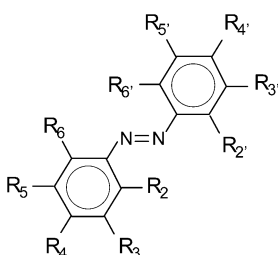
In this paper, we report density functional theory (DFT) calculations for ground and excited states and the corresponding anions and cations of azobenzene and various azobenzene derivatives, to explore their possible role in the course of a STM-induced switching process, and, to a lesser extent, also of photoinduced reactions. This includes the characterization and the control (by substitution), of the anion and cation states, computation of possible reaction pathways and barriers along them, and the estimation of field effects. While the calculations are done for isolated molecules, the energetics and electronic structure are discussed in light of published and ongoing STM switching experiments. This is a necessary first step toward a more complete treatment which explicitly accounts for surface effects. It has already been checked, however, by preliminary cluster calculations in which a few gold atoms were considered, that charge transfer between the surface and azobenzenes noncovalently attached to it can be expected to be small.

2. Molecules and Computational Details

The molecules studied in this work are tabulated in Table 1, with the notation for substituents chosen according to the numbering of atoms to which they are attached. Besides the azobenzene molecule (henceforth AB), several double-substituted azobenzenes such as DMC, CMA, and DO3 and TTA were considered. Also, an isomer of CMA, PCMA, with carboxymethyl groups in para instead of meta positions, and, for the trans form, also the para-substituted dicyano compound (DPC), was studied. The choice of molecules was motivated by the STM experiments and by the goal to investigate the influence of different types of substituents in various positions on the electronic structure.

We have used the Gaussian 98²⁷ program package for all calculations. We employed the B3LYP²⁸ hybrid functional of DFT for all ground state calculations and the TD-DFT²⁹ method with the same functional for excited states. For the calculation of stationary points (done for all molecules), and of the relaxed potential energy curves and vertical electron affinities (which were done for selected molecules), a 6-311G**^{30,31} basis set was used. An exception is TTA, for which only a 6-31G* basis set^{32–34} was employed. The 6-31G* basis set was also used for all two-dimensional potential energy surfaces, which were

TABLE 1: Schematic Representation of the Investigated Molecules: Azobenzene (AB), Dimetacyano-azobenzene (DMC), 3,3'-Carboxymethylester-azobenzene (CMA), 4,4'-Carboxymethylester-azobenzene (PCMA), Disperse Orange 3 (DO3), and 3,3',5,5'-Tetra-*tert*-butyl-azobenzene (TTA)



	R_3	R_4	R_5	R_5'	R_4'	R_3'
AB	H	H	H	H	H	H
DMC	CN	H	H	CN	H	H
DPC	H	CN	H	H	CN	H
CMA	COOCH ₃	H	H	H	H	COOCH ₃
PCMA	H	COOCH ₃	H	H	COOCH ₃	H
DO3	H	NH ₂	H	H	NO ₂	H
TTA	<i>tert</i> -butyl	H	<i>tert</i> -butyl	<i>tert</i> -butyl	H	<i>tert</i> -butyl

computed for selected molecules. Test calculations were also performed with diffuse basis sets 6-311+G** 6-311++G**,³⁵ and with correlated wave-function-based methods.

Below, we shall calculate stationary points, and also one-dimensional “reaction paths” along the rotational angle, ω , which is shown in Figure 1 with all other degrees of freedom

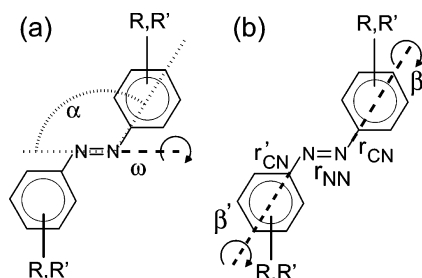


Figure 1. Shown are the coordinates involved in the potential energy surface (PES) calculations. The two angles α and ω , shown in part a, are varied to obtain the PES. All other internal coordinates are kept fixed, except the three bond lengths r_{NN} , r_{CN} , r'_{CN} and the two dihedral angles β and β' , shown in part b, which are relaxed during the calculations.

reoptimized. For 2D potential energy surfaces, for the ground state surface, the inversion angle, α (see Figure 1), and the rotation angle, ω , were varied starting from the equilibrium geometry of the cis isomer. All other internal coordinates were kept fixed in this case, except the three bond lengths r_{NN} , r_{CN} , and r'_{CN} and the two dihedral angles β and β' , as defined in Figure 1. The *inversion* and *rotation* pathways are considered in this work. These are possible modes for isomerization of azobenzenes after photoexcitation to the S_1 ($n \rightarrow \pi^*$ excitation) and S_2 ($\pi \rightarrow \pi^*$ excitation) states, respectively. This is an idealization, since other, more complicated reaction pathways and coordinates for photochemical isomerization of neutral azobenzenes have been suggested recently,^{4,10,22} as well as the possible importance of other excited states, such as the triplet T_1 .⁸

3. Results and Discussion

3.1. Neutral Azobenzene and Method Testing. We computed the equilibrium geometries of all investigated azobenzene derivatives, shown in Table 1, for the neutral molecules and

TABLE 2: Selected Geometry Parameters for AB (left) and Vertical Excitation Energies from S_0 to the First Lowest Excited Singlet States S_1 and S_2 (right), with Oscillator Strengths, f , in Parentheses^a

	ω (deg)	α (deg)	r_{NN} (Å)	r_{CN} (Å)	S_1 (eV) (f)	S_2 (eV) (f)
cis						
(TD)-B3LYP	9.8	124.9	1.243	1.436	2.59 (0.036)	4.17 (0.069)
MP2/CCSD ²	7.3	120.8	1.261	1.432	3.17	4.67
exptl	8.0 ^b	121.9 ^b	1.253 ^b	1.449 ^b	2.92 ^c	4.4 ^d
trans						
(TD)-B3LYP	180	114.8	1.253	1.418	2.54 (0.000)	3.81 (0.775)
MP2/CCSD ²	180	113.7	1.268	1.417	2.95	4.36
CASSCF ⁴					3.11	5.56
exptl	180 ^b	113.6	1.247	1.428	2.82 ^c	4.12 ^c

^a Given are the values for the optimized angles, α and ω , the N–N bond length, r_{NN} , and the C–N Bond Length, r_{CN} . The (TD)-B3LYP values are taken from this study and compared to high-level ab initio calculations at the MP2/cc-pVTZ level of theory for ground state geometries,² and CCSD for excited states.² Also, experimental values are given for comparison. For the trans form, also selected CASSCF calculations are reported.⁴ ^b From X-ray measurements.^{45,46} ^c From gas phase spectroscopy.⁴⁷ ^d From spectroscopical data in ethanol.⁴⁸

the corresponding anions in both the cis and trans configurations. For selected molecules, we have also considered cationic species. We focus on the anionic species in the following, as possible intermediates for STM-induced isomerization at a surface, at a positive sample bias.

In Table 2, some results for unsubstituted azobenzenes are given and compared to high-level ab initio and experimental data. Both the α and ω angles and the N–N and C–N bond lengths are well reproduced by the B3LYP/6-311G** calculations compared to the wave-function-based ab initio and experimental values.

Also, the excitation energies to S_1 and S_2 are reasonable, which are underestimated by roughly 10% on the TD-B3LYP/6-311G** level of theory. CCSD excitation energies, on the other hand, are somewhat too large. CASSCF excitation energies are much too large when compared to experiment. The (TD)-B3LYP method is thus found to offer, for azobenzenes, reasonable accuracy at comparatively low cost, in agreement with earlier studies.^{2,4}

For the trans isomer, the $S_0 \rightarrow S_1$ transition is dominated by a highest occupied molecular orbital (HOMO) \rightarrow lowest unoccupied molecular orbital (LUMO) transition, where the HOMO consists dominantly of the N lone pairs and the LUMO is dominated by the π^* orbital of the NN moiety, with some contributions from the p_z orbitals of carbon atoms in ortho and para positions. The $S_0 \rightarrow S_2$ transition is essentially a HOMO-1 \rightarrow LUMO transition, where the HOMO-1 is dominated by the π orbital of the NN unit. The three frontier Kohn–Sham orbitals, π = HOMO-1, n = HOMO, and π^* = LUMO orbitals are illustrated in Figure 2. Note that the $n \rightarrow \pi^*$ transition is symmetry forbidden; hence, the oscillator strength is zero, while $\pi \rightarrow \pi^*$ is strongly allowed. Both transitions are allowed for the cis isomer, albeit the $\pi \rightarrow \pi^*$ transition now with a smaller oscillator strength.

3.2. Neutral Substituted Azobenzenes. The geometries and many other properties of the substituted azobenzenes are similar to those of azobenzene. Table 3 gives a summary, showing the dipole moment, $|\mu|$, the energy difference between cis and trans, $\Delta E = E_{\text{cis}} - E_{\text{trans}}$ (trans is always more stable), and the activation energy for isomerization, E^\ddagger , along ω (see below), for the cis and trans forms.

That the structures shown are minima on the potential energy surface was checked by normal-mode analysis which gave only

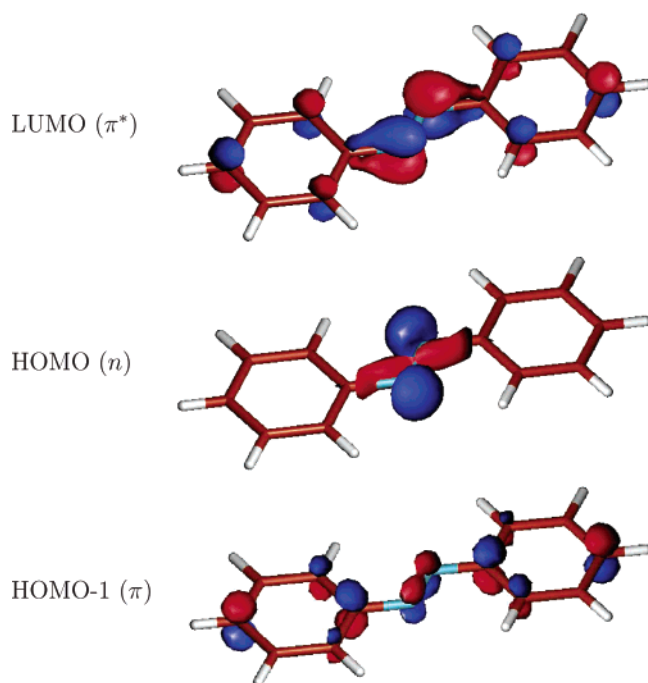


Figure 2. Kohn–Sham B3LYP/6-311G** frontier orbitals of *trans*-azobenzene.

real frequencies. The substituted molecules have all very similar geometries for the azobenzene backbone. For all investigated (symmetrically substituted) azobenzenes, we get $r_{\text{NN}} \approx 1.24$ Å and $r_{\text{CN}} \approx 1.44$ Å for the *cis* isomers and $r_{\text{NN}} \approx 1.26$ Å and $r_{\text{CN}} \approx 1.42$ Å for the *trans* isomers, with maximal deviation from these mean values of only 0.01 Å. Also, the angles ω and α show only a very small dependence on the substituents, with ω varying between 7 and 10° for the neutral *cis* isomers. Even less affected is α , which is around 124.5° for the *cis* isomers and 115° for the *trans* isomers, with a maximal deviation from these mean values of 0.5°. For DO3, due to its asymmetric substitution, there are two different CN bond lengths, r'_{CN} (closer to NH_2) and r_{CN} (closer to NO_2), and angles, α' and α . For *cis*, $r'_{\text{CN}} \approx r_{\text{CN}} = 1.42$ Å, $\alpha' = 125^\circ$, and $\alpha = 126^\circ$. For *trans*, $r'_{\text{CN}} = 1.40$ Å, $r_{\text{CN}} = 1.41$ Å, $\alpha = 115^\circ$, and $\alpha' = 116^\circ$.

Apart from nonplanar sidegroups, all molecules considered here are planar in their *trans* forms. All *cis* forms are three-dimensional and have a large dipole moment also in cases when the *trans* molecules have none. For the *cis* molecules, the dipole moment is dominantly oriented perpendicular to the NN axis. The largest dipole moment is found for the push–pull compound DO3, in its *trans* form, oriented roughly parallel to the NN axis, with the NH_2 end positively charged and the NO_2 end negatively charged.

Note that for certain molecules also other stable configurations than those shown are possible. For example, the *trans* form of DMC shown can be classified as *trans–trans*, since also the CN groups are *trans* oriented. There is also a *trans–cis* form with the CN groups in *cis* orientation. The *trans–cis* form was found to be only by about 0.01 eV less stable than the *trans–trans* form, at both the B3LYP/6-311G** and MP2/6-311G** levels of theory. Also, other properties are similar, with the exception of the dipole moment which is $|\mu| = 7.598$ D for *trans–cis*. Similarly, the *trans–cis* CMA molecule shown has a nonvanishing dipole moment.

While the energetic differences between the *cis* and *trans* forms are similar for all molecules, $\Delta E \sim 0.7$ eV, there is a great variation of the activation energy with respect to *cis* →

trans (and *trans* → *cis*) isomerization, in the neutral ground state. The *trans* → *cis* activation energies, along a relaxed path along the ω angle, varies from about 1.4 eV (DO3) to more than 2 eV (AB). The corresponding *cis* → *trans* activation energies are always by ΔE smaller but still large. It should be noted that the ground state barriers in particular along ω are not very accurate at the B3LYP level of theory. The theoretical treatment here neglects the mixing in of higher excited singlet states (and a triplet state⁸) along ω ; that is, static correlation is important and not well treated by B3LYP. More importantly, rotation alone is not the relevant reaction path^{4,10,22} and therefore the true ground state barrier is overestimated. Experimentally, one finds an isomerization barrier for azobenzene on the order of 1 eV.¹⁴

3.3. Anionic Azobenzenes. As possible intermediate states for resonant STM switching at positive sample bias, anionic species of azobenzenes were considered. In Table 4, the electron affinities of these compounds, that is,

$$\text{EA} = E(\text{A}) - E(\text{A}^-) \quad (1)$$

are shown. We distinguish between vertical (no geometry reoptimization for the anionic species A^-) and relaxed electron affinities (with geometry reoptimization). For dicyano-azobenzene, not only the meta-substituted species (DMC) but also the para-substituted species (DPC) was considered, in the *trans* configuration.

The vertical and relaxed electron affinities given in Table 4 vary for a given isomer (*cis* or *trans*), over a range of about 2 eV. As expected, the lowest EA values are found for the alkyl-substituted species TTA and the highest EA values for molecules with only electron-withdrawing groups such as CN.

For anions, diffuse basis functions are usually required for accurate predictions. To check this for selected azobenzene species, the vertical electron affinity for the *trans* form was recalculated with the 6-311+G** and 6-311++G** basis sets, with one or two sets of diffuse functions added. With these basis sets, the electron affinity increases by about 0.2 eV for both bases, as indicated in Table 4 for selected molecules in the *trans* form. This is then also the approximate value by which we systematically underestimate electron affinities when using 6-311G** (or 6-31G* as for TTA).

There is a stronger effect due to the position of the substituents. By comparison of DMC and DPC, and also of CMA and PCMA, it is seen that para substitution leads to electron affinities which are by up to almost 0.5 eV larger than those for meta substitution. This can easily be understood from Figure 2, according to which the LUMO of the neutral (*trans*) molecule has a nonvanishing contribution at the para positions but a node at the meta positions. Electron-withdrawing substituents in the para position rather than the meta position will therefore lead to a stronger energetic stabilization of the LUMO. In the sense of Koopmans' theorem for electron affinities³⁶ (which is not strictly valid for Kohn–Sham orbitals, though), one might expect a linear relationship between EA and the negative of the LUMO energy, $\text{EA} \approx -\epsilon_{\text{LUMO}} + A$, where A is a measure for the orbital relaxation and the larger correlation energy of the anion. This expectation is nicely fulfilled according to Figure 3, where an almost linear relationship is demonstrated for the *trans* azobenzenes considered in this work.

Placing (for the dicyano species) the substituents in the ortho positions of the benzene ring gave only a small enhancement of the electron affinity (by less than 0.1 eV), relative to meta substitution. Again, this can qualitatively be understood from the topology of the LUMO, with smaller coefficients in ortho than para positions.

TABLE 3: Molecules Considered in This Work, with Optimized Structures Shown, and Corresponding Properties: Modulus of Dipole Moment, $|\mu|$, Energy Difference between the cis and trans Forms, ΔE , and Activation Energy for Isomerization, E^\ddagger (along ω , See Below) (All Calculations Were Done at the B3LYP/6-311G Level of Theory, except for TTA, Which Was Done at the B3LYP/6-31G* Level)**

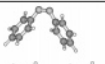
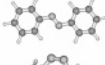

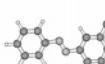
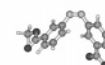
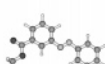
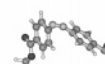
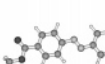

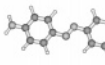

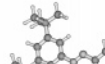
	molecule		$ \mu $ (Debye)	ΔE [eV]	E_{iso}^\ddagger [eV]
AB	cis		3.211	0.68	1.37
	trans		0		2.05
DMC	cis		6.983	0.71	1.03
	trans (-trans)		0		1.80
CMA	cis		3.210	0.68	1.10
	trans (-cis)		3.009		1.78
PCMA	cis		3.240	0.66	1.03
	trans		0.		1.69
DO3	cis		7.541	0.71	0.73
	trans		9.870		1.44
TTA	cis		3.600	0.65	1.39
	trans		0.001		2.04

TABLE 4: Vertical and Relaxed Electron Affinities, EA, and the Energy Differences, ΔE , between the cis and trans Configurations for the Investigated Azobenzene Derivatives^a

	AB	DMC	DPC	CMA	PCMA	DO3	TTA
EA (cis, vertical)	0.43	1.38		0.79	1.82	1.12	0.11
EA (cis, relaxed)	1.01	1.94		1.34	1.84	1.42	0.72
EA (trans, vertical)	0.81	1.73	2.08	1.17	1.60	1.44	0.52
	(1.01)	(1.91)		(1.37)	(1.80)	(1.71)	
EA (trans, relaxed)	1.05	1.97	2.30	1.42	1.89	1.69	0.76
ΔE (neutral)	0.68	0.71		0.68	0.66	0.71	0.65
ΔE (anion)	0.73	0.75		0.76	0.71	0.75	0.69

^a The trans isomer is the most stable one in all cases. For DPC, only the trans form was calculated. All calculations were done with the 6-311G** basis set, except for TTA, where 6-31G* was used. To check the role of diffuse functions, for selected molecules, the vertical EA of the trans form was calculated with 6-311+G** and 6-311++G**. The results are very similar for both bases, with the values for the better one given in parentheses under EA (trans, vertical). All values are in eV.

The results indicate, that one can “tune” the affinity levels by substitution. Moreover, it is found that, for the anions, the cis isomers are further destabilized compared to the neutral

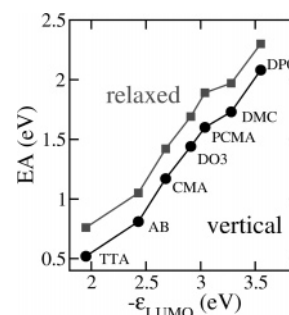


Figure 3. Shown are the computed vertical and relaxed electron affinities (eq 1) in correlation to $-\epsilon_{LUMO}$, for all trans molecules considered in Table 4. The EA/ $-\epsilon_{LUMO}$ for TTA is probably too small due to the smaller basis set used for this molecule.

molecules, relative to the trans isomers. This destabilization may be due to electrostatic repulsion between the two phenyl groups in the anion.

Concerning the relaxed geometries of the anionic species, one observes a pronounced change in some of the bond lengths

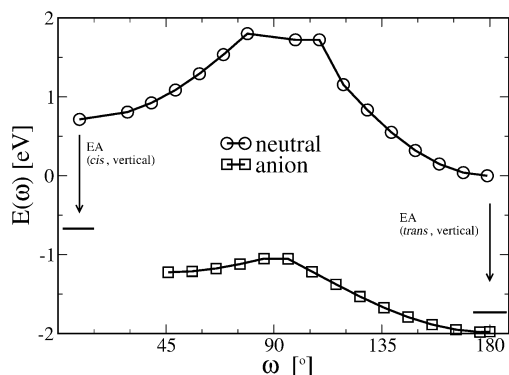


Figure 4. Shown are the potential energy curves obtained from a fully relaxed scan along ω from the cis to the trans isomer for the neutral DMC molecule (circles) and the DMC anion (squares). Also indicated are the energies related to the vertical electron affinities of the neutral equilibrium geometries.

and angles compared to the neutral molecules. For the cis and trans forms, the NN bond length is elongated in the anion, by ≈ 0.07 Å for *trans*-azobenzene and ≈ 0.09 Å for *cis*-azobenzene. This is mostly due to the fact that the LUMO of the neutral molecule, which is N–N antibonding, is occupied in the anion. For the same reason, the dihedral angle, ω , that is, the angle describing the rotation pathway, changes from ≈ 9 to $\approx 46^\circ$ in the cis isomers. (The trans isomers remain planar.) Since the inversion angles, α , remain largely unaffected, this indicates that upon electron attachment the molecule will tend to rotate around ω (see below). By the attachment process, also the CN bond shortens, by about 0.05 Å for *trans*-AB and 0.07 Å for *cis*-AB, since the LUMO of the neutral molecule is C–N bonding.

3.4. Relaxed Potential Energy Curves. To explore the possibility of an electron mediated switching from trans to cis and vice versa along ω in more detail, we computed fully relaxed potential energy curves along ω for the neutral and the negatively charged molecules. As a representative example, the curves for DMC are shown in Figure 4. The upper curve (circles) is for the neutral molecule, and the lower one is for the anion, with the energy zero chosen as the energy of the neutral trans form. On a surface, this energetic order will most probably change, because one needs to add the work function of the surface or the tip, Φ , and correct for image charge stabilization of the anion:

$$V_A^-(\omega) - V_A(\omega) = -EA(\omega) + \Phi + \Delta_{\text{im}} \quad (2)$$

Without the latter two terms, which will be estimated below, the anion curve in Figure 4 is obtained, shown here in the range from one minimum (cis, at $\omega \approx 46^\circ$) to the other (trans, at $\omega = 180^\circ$). The vertical electron affinities for the *cis*- and *trans*-DMC are indicated by horizontal dashes and vertical arrows.

One recognizes that by occupation of π^* not only does ω substantially widen in the anionic cis configuration, but also, the barrier for the isomerization is greatly reduced, from 1.03 to 0.18 eV. Also, the barrier for the trans–cis reaction is lowered from 1.80 to 0.93 eV, indicating a much weaker N–N double bond in the anion. One can also see that an anion, formed by vertical electron attachment in the cis configuration, would have an energy above the barrier for isomerization along ω .

The relaxed potential energy curves for the other molecules are very similar to the one of DMC. The barriers derived from these curves for some of the molecules are given in Table 5, except for the anionic AB state, for which we were unable to obtain a stable relaxed scan. One can see that also for the other

TABLE 5: Barriers for the cis \rightarrow trans Isomerization, E_{cis}^+ , and the trans \rightarrow cis Isomerization, E_{trans}^+ , along the Angle ω (Rotation Mechanism), Obtained from the Relaxed Potential Energy Curves^a

	AB	DMC	CMA	PCMA
neutral				
E_{trans}^+	2.05	1.80	1.78	1.69
E_{cis}^+	1.37	1.03	1.10	1.03
anion				
E_{trans}^+		0.93	0.94	0.91
E_{cis}^+		0.18	0.16	0.20

^a All values are in eV. For the anionic curve of AB, no convergence was achieved.

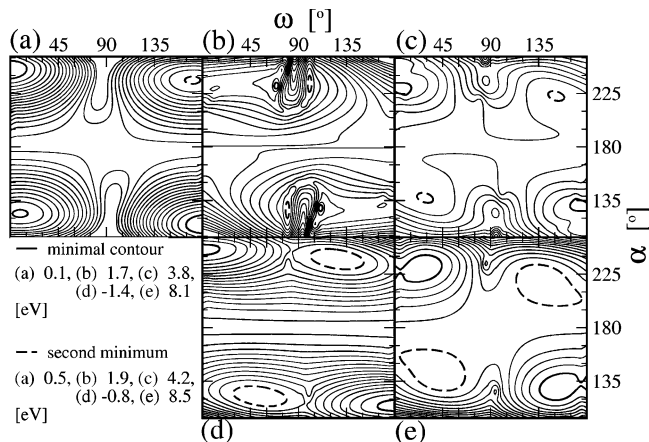


Figure 5. Shown are contour plots obtained by spline interpolation of the calculated PES for the DMC molecule: (a) for the ground state; (b) for the S_1 state; (c) for the S_2 state; (d) for the anion; (e) for the cation. The bold contour encloses the global minimum on each surface, and the dashed one is the second most stable configuration. All contours are separated by 0.1 eV, and all energies are given relative to the global minimum of the PES for the neutral molecule, that is, the trans isomer.

azobenzene derivatives the barrier is much smaller in the anionic state than in the neutral ground state. Additionally, for all substituted azobenzenes, except PCMA, the barrier for the cis \rightarrow trans reaction is smaller than the difference between the vertical and relaxed electron affinities, indicating spontaneous cis \rightarrow trans isomerization in the anionic state. In general, anion formation will greatly enhance the probability for switching of azobenzenes, along ω .

3.5. Potential Energy Surfaces. Potential energy surfaces for selected neutral molecules (AB, DMC, CMA, and PCMA) in their ground state, along the “rotation” and “inversion” modes ω and α , were calculated as described in section 2. For the anionic, the cationic, and the neutral excited state potential energy surfaces (PESs) S_1 and S_2 , the coordinates r_{NN} , r_{CN} , r'_{CN} and angles β and β' of Figure 1, as optimized for each point (ω , α) of the ground state, were used. This means we restrict ourselves to vertical transitions from the ground state, other than the reaction paths along ω in Figure 4, which refer to fully relaxed scans. For DMC, we used 37 points in ω from 0 to 180° and 15 points in α from 104.1 to 174.1° , that is, 555 points in total. The PESs for the other molecules were calculated with a sparser grid consisting of 8 points in α and 18 in ω , that is, in total 144 points.

The surfaces for DMC are shown in Figure 5, for (a) the ground state S_0 , (b) the S_1 state, (c) the S_2 state, (d) the anionic state A^- , and (e) the cationic state A^+ . Considering the ground state S_0 , we note minima corresponding to the trans ($\omega = 0^\circ/180^\circ$, $\alpha \approx 115^\circ/245^\circ$) and cis ($\omega = 10^\circ/170^\circ$, $\alpha \approx 125^\circ/235^\circ$)

TABLE 6: Barriers for the trans \rightarrow cis Isomerization, $E_{\text{trans}}^{\ddagger}$, for the Rotation Mechanism (Motion Mainly along ω) and the Inversion Mechanism (Motion Mainly along α), as Obtained from the 2D Potential Energy Surfaces (All Values Are in eV)

	DMC	CMA	PCMA
rotation (ω)			
$E_{\text{neutral}}^{\ddagger}$	2.24	1.94	2.15
$E_{\text{anion}}^{\ddagger}$	0.54	0.76	0.69
$E_{\text{cation}}^{\ddagger}$	0.80	0.75	0.95
inversion (α)			
$E_{\text{neutral}}^{\ddagger}$	1.72	1.63	1.55
$E_{\text{anion}}^{\ddagger}$	1.66	1.50	1.48
$E_{\text{cation}}^{\ddagger}$	0.25	0.01	0.26

configurations. Connecting the trans and cis minima around $\alpha \approx 120^\circ$, mainly along ω , gives approximately, but not exactly, the reaction path shown as the upper curve of Figure 4. The reaction barrier for geometry-restricted trans \rightarrow cis isomerization along ω , $E_{\text{neutral}}^{\ddagger}$, is 2.24 eV (see Table 6), which is somewhat higher than the fully relaxed barrier of 1.80 eV according to Table 5. Isomerization from trans to cis around $\omega \approx 180^\circ$ mainly along α , on the other hand, requires an energy of only 1.72 eV according to Table 6 on the restricted 2D surface.

While the 2D ground state barriers are overestimated due to the geometry restrictions, a relatively small basis set, and due to missing static correlation, they appear to be too large to be overcome thermally. Rather, electronic excitation is required. In the S_1 state of the neutral molecule, there is a large gradient in α and ω in the Franck–Condon regions for both the cis and trans isomers. Around $\omega = 90^\circ$, one can see two local minima separated by a barrier, which is a signature of a conical intersection⁴ that leaves its traces also in S_0 , which is nonsmooth in that region (see Figure 4). Therefore, an excitation to S_1 should lead to an isomerization for both isomers in a combined motion in α and ω . Note that, optically, the S_1 state can only be reached out of the cis configuration, at least if vibronic effects are neglected. This selection rule does not necessarily apply to nonoptical transitions, and to molecules adsorbed at surfaces where the molecule will be distorted. The situation is less clear for the S_2 state. Although there are also nonvanishing gradients at the Franck–Condon points, we have local minima nearby for the cis and trans configurations, which disfavor the isomerization dynamics. The topology of the (ω , α) surfaces of S_0 and S_1 is similar to that for azobenzene, as reported in ref 3, based on CASSCF. Some differences occur for the S_2 surface. In ref 1, a clear minimum was found along ω for S_2 . It may well be that TD-DFT has difficulties to represent this state correctly.^{7,11}

It is generally to be noted that the (photo)excited azobenzenes are only short-lived intermediates, with $S_2 \rightarrow S_1$ and $S_1 \rightarrow S_0$ internal conversion occurring on a sub-picosecond time scale.⁴ It is also known that two other $\pi\pi^*$ excited states S_3 and S_4 are located energetically close to S_2 .⁴ The exact relaxation pathway, for example, rotation or inversion, both or neither of them, is still under discussion.⁴ At metal surfaces, electronic quenching is expected to be even faster, with lifetimes on the order of a few femtoseconds being typical. As a consequence, the excited potential sets atoms only in motion, while switching is expected to happen after quenching, in the ground state.

Considering the anionic surface in Figure 5d, one can draw the same conclusions as those drawn from the relaxed potential energy curves in the previous sections (Figure 4). The barrier for the cis–trans isomerization is greatly reduced in ω , and the potential energy gained after a vertical transition should be

enough to overcome this barrier, even when still in the anion state. For the cationic surface, not only the barrier in ω is reduced but even more so the one in α . Nevertheless, like the S_2 surface, we have two pronounced local minima for the cis and the trans isomer, which makes the direct isomerization in this state unlikely. However, also the ionic states are short-lived resonances at a metal surface at least, and isomerization is expected to be possible in the ground state after transient population of positive and negative ion states and quenching.

The barriers for trans \rightarrow cis isomerization extracted from the restricted 2D PESs of the different azobenzene derivatives are given in Table 6. One can see that in all cases ionization of the molecule leads to a reduction of the barriers for both isomerization mechanisms. However, for the anion, this reduction for the inversion mechanism is rather small.

3.6. Further Discussion in Relation to STM Experiments.

Some of the above results have already been discussed with respect to their possible significance for STM-induced switching. A few further aspects will be discussed now.

3.6.1. Threshold Behavior. Let us first recall the experiments of ref 26, where switching (and desorption) at a positive sample bias was observed for DMC and CMA on Au(111). For DMC/Au, the switching, probably from trans, occurred above a voltage threshold of about 1.6 eV, while the threshold for CMA was at around 2.3 eV. It was speculated that the reaction proceeds through a “negative ion resonance” state, that is, by electron attachment to the LUMO of the molecule.

This interpretation is supported by the present calculations. Our starting point is eq 2, which gives the excitation energy for negative ion resonance formation, as a function of ω . To make a very rough estimate, for Φ , we take the work function of gold (≈ 4.6 eV) and the image charge stabilization as $\Delta_{\text{im}} \approx -e^2/4Z \approx 1.2$ eV corresponding to an anion–image hole distance, Z , of ≈ 3 Å. We thus obtain for DMC/Au an excitation energy of $V_{\text{A}}(\omega) - V_{\text{A}}(\omega) \approx (-1.73 + 4.6 - 1.2)$ eV ≈ 1.7 eV for vertical excitation out of the trans configuration. [The nonvertical excitation energy would be by about 0.26 eV lower (see Table 4). An additional 0.2 eV may come from the inaccuracy of the 6-311G** basis set for electron affinities (see above)]. For CMA/Au, on the other hand, we estimate a vertical excitation energy of $(-1.17 + 4.6 - 1.2)$ eV ≈ 2.2 eV by the same token. Assuming that the energy is provided by sudden attachment of a single electron with an energy “above threshold”, these values correspond nicely to the threshold voltages found in experiment. If this picture is correct, we predict from the calculations reported in Table 4 that PCMA, that is, the para-substituted carboxymethyl species, will switch out of the trans form at about $(-1.60 + 4.6 - 1.2)$ eV ≈ 1.8 eV, similar to DMC.

In passing, we note that the exact outcome of the reaction of DMC on Au(111) is not yet known. When starting from trans–trans DMC, for example, both the cis and the trans–cis forms could be reached, the latter by rotation about the angle β (see Figure 1b). The calculated torsional barrier for the trans–trans \rightarrow trans–cis isomerization is 0.31 eV for neutral DMC and 0.60 eV for DMC[−]. The fact that the rotation in the anion state is now hindered in comparison to the neutral molecule can again be rationalized qualitatively from inspection of the LUMO π^* of the neutral molecule (see Figure 2), which is weakly bonding between the central N and C atoms. The learning from this calculation is that the barrier for rotation around β is small in comparison to rotation around ω and inversion along α , in particular in the ground state. Of course, on a surface, these barriers are expected to be different. Still, rotation around β

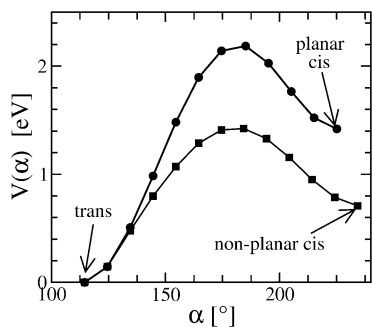


Figure 6. Relaxed potential energy curve $V(\alpha)$ for inversion of DO3, at the NO_2 side, along the inversion angle, α . All other internal coordinates were, apart from the planarity constraint, relaxed during the calculations. Upper curve, unconstrained molecule; lower curve, molecule constrained to remain planar.

appears as an alternative reaction pathway, possibly already at lower threshold voltages.

3.6.2. Inversion of DO3. In ref 37, the observed STM cis–trans isomerization of DO3 on Au(111) has been assumed to be caused by inelastically scattering tunneling electrons which drive, in the electronic ground state, the reaction from trans to planar cis and vice versa, through inversion along α . The rotation along ω was considered unlikely for an azobenzene chemisorbed on a metal surface. In ref 37, it was argued that in a planar cis form the α angle is widened initially, to minimize the steric repulsion of the two phenyl rings. This is consistent with an observed increase of $\alpha \approx 127^\circ$ for the gas phase to $\alpha \approx 150^\circ$ on the surface.³⁷ It was argued that for a planar cis form the barrier for inversion might be much lower, thus explaining the low threshold of about 650 meV (rather than 1.6 eV according to ref 26) for trans \rightarrow cis isomerization and ≤ 640 meV for cis \rightarrow trans switching.

We checked these conjectures by gas phase DFT calculations, in which DO3 was forced to remain planar. By geometry optimization, it is found that for cis α angle (inversion angle at the NO_2 side) widens from 126° to $\alpha = 138^\circ$ in the planar configuration, and similarly α' (NH_2 side) widens from 125° to $\alpha' = 135^\circ$. Thus, the trend described in ref 37 is confirmed. In further agreement with expectation, there is a pronounced energy shift upward of the planar form: the cis–trans energy difference, ΔE , is doubled from 0.71 eV for the nonplanar cis form to 1.42 eV in planar cis-DO3. On the other hand, the inversion barrier for cis \rightarrow trans isomerization is *not* much affected when planarity is enforced. This is demonstrated in Figure 6, where the fully relaxed potential energy curves $V(\alpha)$ for inversion of the NO_2 side of DO3 along the angle α are shown, for the unconstrained molecule (upper curve) and the planar molecule (lower curve).

For the nonplanar molecule, the inversion barrier is about 0.7 eV for the cis \rightarrow trans isomerization and about 1.4 eV for the other direction. For planar DO3, on the other hand, the cis \rightarrow trans isomerization barrier is also around 0.7 eV, and the barrier in the reverse direction is more than 2.1 eV. In fact, the activation energy for trans \rightarrow cis isomerization cannot be lower than ΔE , the energy difference between cis and trans forms, and should therefore be larger than that for the unconstrained molecule.

If the hypothesis of ref 37 holds, therefore, we expect a large asymmetry between ground state barriers for the cis \rightarrow trans and the trans \rightarrow cis directions, respectively. We should also expect that the energy for surmounting the ground state barrier for the trans \rightarrow cis reaction cannot come from a single ≈ 650 meV electron. At least three electrons would be required instead.

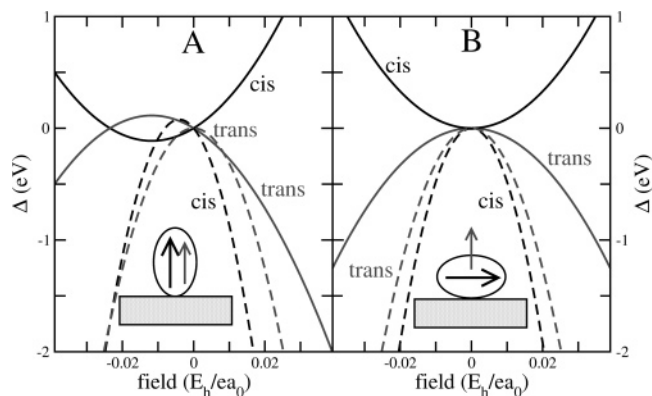


Figure 7. $\Delta V(\text{cis})$ and $\Delta V(\text{trans})$ (dashed) and $\Delta E^\ddagger(\text{cis})$ and $\Delta E^\ddagger(\text{trans})$ values (solid) calculated for TTA within models A and B. Indicated as sketches are, for the cis form, the orientation of the permanent (thick arrow) and the induced dipole moment (thinner arrow) relative to the surface (see text). The energies are given in electronvolts, and the field strength is given in atomic units. Note that $0.01 E_h/ea_0$ corresponds to 0.51 V/\AA .

In contrast, it seems possible that a single ≈ 650 meV electron may enforce the cis \rightarrow trans reaction. Of course, the situation may be different when DO3 is adsorbed on a metal surface. However, it is to be expected that flat DO3 interacts with its π system with the surface in similar ways for the cis, trans, and transition-state-like conformations, thus shifting the potential energy curve as a whole. The present calculations suggest that the interpretation of the STM experiments in ref 37 may not be quite complete.

3.6.3. Field Effects. Field effects may play some role for STM-induced switching of substituted azobenzenes, such as TTA.²⁵ Due to its bulky substituents, the molecule interacts only weakly with the surface, by physisorption. An external electric field will distort the ground state potential, leading to different reaction energies and energy barriers. To estimate these effects, we assume that the STM tip gives rise to a homogeneous field, F_z , along z . Neglecting any other field components, field inhomogeneities, and higher-order polarizabilities, an effective potential along a set of coordinates, q , can be defined as

$$V(q) = V_0(q) - \mu_z(q)F_z - \frac{1}{2}\alpha_{zz}(q)F_z^2 \quad (3)$$

Here, V_0 is the field-free ground state potential, μ_z the z -component of the permanent dipole moment, and α_{zz} the zz -component of the polarizability tensor, where z is the direction perpendicular to the surface.

Since we do not know how the molecule is oriented relative to surface and tip, we make some model assumptions. It is reasonable to assume that the trans form lies flat on the surface with the NN axis and phenyl rings parallel to it. For the cis form, we assume in the first model, A, that both the permanent molecular dipole and the induced molecular dipole are perpendicular to the surface, that is, aligned with the field (see the inset of Figure 7A). In model B, we assume that the permanent dipole is always parallel to the surface and only the induced dipole moment has a perpendicular component (see the inset of Figure 7B). Within both of these models, eq 3 gives energy shifts for the cis and trans forms relative to the field-free case of

$$\Delta V(\text{cis}) = -\mu_c F_z - \frac{\alpha_c}{2} F_z^2 \quad (4)$$

$$\Delta V(\text{trans}) = -\frac{\alpha_{\perp}}{2} F_z^2 \quad (5)$$

In eq 4, μ_c is the permanent dipole perpendicular to the surface. In model A at a positive sample bias ($F_z > 0$), the field is parallel to the permanent dipole moment, μ_c , thus stabilizing the molecule in the cis form. Further, α_c is the relevant matrix element of the polarizability tensor, that is, $\alpha_c = \alpha_{\perp,c}$ in model A, where $\alpha_{\perp,c}$ is the zz -element of the diagonalized polarizability tensor (see below).

In model B, the permanent dipole is $\mu_c = 0$ and $\alpha_c = \alpha_{\parallel,c}$. Here, $\alpha_{\parallel,c}$ is a component of the polarizability tensor creating an induced dipole perpendicular to the surface but parallel to the NN axis, which was estimated from diagonalizing the polarizability tensor and defining

$$\alpha_{\parallel} = \frac{1}{2}(\alpha_{xx} + \alpha_{yy}) \quad (6)$$

Finally, in eq 5, α_t is the zz -component of the polarizability tensor of the trans form; when the latter lies flat on the surface, $\alpha_t = \alpha_{\perp,t}$. For TTA, we obtain for various contributions to the polarizability the 6-31G* values, as given in Table 7.

One notes that *trans*-TTA has, as expected, a larger polarizability parallel to the NN axis, that is, parallel to the benzene rings with their mobile π -electrons, rather than perpendicular to the molecular plane. For the cis form, being more three-dimensional, α_{\parallel} and α_{\perp} are more similar to each other. Both are larger than α_{\perp} of the trans form, and thus, the cis isomer will be stabilized by vertical polarization to a larger extent than the trans form, in both models. For model A, however, the cis form can also be destabilized if the permanent dipole moment is antiparallel to the external field. The situation is illustrated in Figure 7, where $\Delta V(\text{cis})$ and $\Delta V(\text{trans})$ are shown, for various field strengths, as dashed lines.

To estimate activation barriers in the presence of a field, we may assume as a first guess that both μ_z and α_{zz} change linearly along a one-dimensional reaction path and the transition state lies exactly halfway along this path. Then, the barrier energy shifts in energy by $[\Delta V(\text{cis}) + \Delta V(\text{trans})]/2$, and the barrier heights encountered from the trans and cis side change according to

$$\Delta E^{\ddagger}(\text{cis}) = \frac{\Delta V(\text{trans}) - \Delta V(\text{cis})}{2} = -\Delta E^{\ddagger}(\text{trans}) \quad (7)$$

In Figure 7, we show $\Delta E^{\ddagger}(\text{cis})$ and $\Delta E^{\ddagger}(\text{trans})$ as solid lines. For model A, we note that the barrier for reaction out of the trans form is always lowered, while the cis \rightarrow trans isomerization requires more energy than in the field-free case. In model A, the trans \rightarrow cis isomerization can be hindered and the reverse process favored, when the permanent dipole is antiparallel to the field.

At this point, a connection to experiment should be made. In ref 25, isomerizations in both directions were found to occur, both at positive and negative sample bias. At least for the trans \rightarrow cis reaction, some asymmetry has been observed, with larger absolute voltages needed to switch the molecule at negative voltage than at positive voltage. This observation is consistent with model A from above, if the permanent dipole of the cis form is oriented such that it is destabilized at $V_s < 0$. On the other hand, such an asymmetry is not clearly seen experimentally for the cis \rightarrow trans isomerization (thus favoring B), and it is also not likely that a pure field effect alone is at work. The latter statement is supported by the fact that very large field

TABLE 7: Polarizabilities of TTA Perpendicular and Parallel to the NN Axis, as Defined in the Text (All Values in Atomic Units, Calculated with B3LYP/6-31G*)

trans		cis	
α_{\parallel}	α_{\perp}	α_{\parallel}	α_{\perp}
455.5	231.4	352.5	300.1
	$=\alpha_t$	$=\alpha_c$ in A	$=\alpha_c$ in B

strengths would be required according to theory. At field strengths around $0.5 \text{ V/\AA} \approx 0.01 E_h/ea_0$, for example, which is not unlike the experimental ones, barriers change on the order of 0.25 eV at most according to Figure 7, which is small in comparison to the field-free barrier of more than 1 eV. To switch the molecule by the field alone, therefore, a field larger by about a factor of 3 is needed. On the other hand, both the permanent dipole and the polarizability can be enhanced at the surface, and details of the molecular orientation as well as the exact variation of these quantities along the (unknown) reaction path were not included in our model. It is also not unlikely that strong fields will lead to a reorientation of the molecule, which is not properly treated here. (In addition, the B3LYP/6-31G* polarizabilities are probably somewhat too small.) Hence, additional work both from experiment and theory is required to address the importance of field effects.

4. Conclusions and Outlook

We presented DFT calculations for azobenzene and substituted derivatives for ground and excited states and the corresponding anions and cations. Although the influence of a surface was only discussed indirectly, our calculations provide strong indications of how a cis–trans isomerization of adsorbed azobenzenes might or might not be enforced by an STM operating in a resonant mode, or through an electric field.

The next step is clearly to describe details of the linking of the molecule to a surface, requiring further quantum chemical calculations. For metal surfaces, this will be somewhat difficult, while semiconductors offer some possibilities here, in particular for excited states. Also, detailed dynamical simulation of switching by inelastic electron tunneling or by field effects is needed in order to get more insight into the possible processes. IET can be treated in the simplest approximation by rate equations.^{38–40} Such models have already been applied to describe vibrational heating, atom transfer in STM experiments, and other phenomena and derive from the more general context of master equation approaches, or approaches which use the full (reduced) density matrix.⁴¹ Reduced density matrix approaches have been used also for above threshold switching.^{42,43} Pure field switching, on the other hand, can be treated in good approximation by wave packet propagation on an effective potential.⁴⁴

Acknowledgment. We thank J. I. Pascual and F. Moresco (both from Freie Universität, Berlin) and their co-workers for fruitful discussions and for sharing experimental results with us prior to publication. We gratefully acknowledge support of this work by the Deutsche Forschungsgemeinschaft through the SFB 658 (subproject C2) and by the Fonds der Chemischen Industrie.

References and Notes

- (1) Cattaneo, P.; Persico, M. *Phys. Chem. Chem. Phys.* **1999**, *1*, 4739.
- (2) Fliegl, H.; Köhn, A.; Hättig, C.; Ahlrichs, R. *J. Am. Chem. Soc.* **2003**, *125*, 9821.
- (3) Ishikawa, T.; Noro, T.; Shoda, T. *J. Chem. Phys.* **2001**, *115*, 7503.

- (4) Schultz, T.; Quenneville, J.; Levine, B.; Toniolo, A.; Martínez, T. J.; Lochbrunner, S.; Schmitt, M.; Shaffer, J. P.; Zgierski, M. Z.; Stolor, A. *J. Am. Chem. Soc.* **2003**, *125*, 8098.
- (5) Cimiraglia, R.; Hofmann, H.-J. *Chem. Phys. Lett.* **1994**, *217*, 430.
- (6) Wei-Guang Diao, E. *J. Phys. Chem. A* **2004**, *108*, 950.
- (7) Gagliardi, L.; Orlandi, G.; Bernardi, F.; Cembran, A.; Garavelli, M. *Theor. Chem. Acc.* **2004**, *111*, 363.
- (8) Cembran, A.; Bernardi, F.; Garavelli, M.; Gagliardi, L.; Orlandi, G. *J. Am. Chem. Soc.* **2004**, *126*, 3234.
- (9) Ciminelli, C.; Granucci, G.; Persico, M. *Chem.—Eur. J.* **2004**, *10*, 2327.
- (10) Toniolo, A.; Ciminelli, C.; Persico, M.; Martínez, T. J. *J. Chem. Phys.* **2005**, *123*, 234308.
- (11) Tiago, M. L.; Ismail-Beigi, S.; Louie, S. G. *J. Chem. Phys.* **2005**, *122*, 094311.
- (12) Ikeda, T.; Tsutsumi, O. *Science* **1995**, *268*, 1837.
- (13) Tamai, N.; Miyasaka, H. *Chem. Rev.* **2000**, *100*, 1875.
- (14) Asano, T.; Okada, T.; Shinkai, S.; Shigematsu, K.; Kusano, Y.; Manabe, O. *J. Am. Chem. Soc.* **1981**, *103*, 5161.
- (15) Fujino, T.; Tahara, T. *J. Phys. Chem. A* **2000**, *104*, 4203.
- (16) Fujino, T.; Arzhantsev, S. Yu.; Tahara, T. *J. Phys. Chem. A* **2001**, *105*, 8123.
- (17) Fujino, T.; Yamaguchi, S.; Tahara, T. *Bull. Chem. Soc. Jpn.* **2002**, *75*, 1031.
- (18) Lu, Y.-C.; Chang, C.-W.; E. Diao, W.-G. *J. Chin. Chem. Soc. (Taipei)* **2002**, *49*, 693.
- (19) Saito, T.; Kobayashi, T. *J. Phys. Chem. A* **2002**, *106*, 9436.
- (20) Satzger, H.; Spörlein, S.; Root, C.; Wachtveitl, J.; Zinth, W.; Gilch, P. *Chem. Phys. Lett.* **2003**, *372*, 216.
- (21) Satzger, H.; Root, C.; Braun, M. *J. Phys. Chem. A* **2004**, *108*, 6265.
- (22) Chang, C.-W.; Lu, Y.-C.; Wang, T.-T.; Diao, E. W.-G. *J. Am. Chem. Soc.* **2004**, *126*, 10109.
- (23) Zhang, C.; Du, M.-H.; Cheng, H.-P.; Zhang, X.-G.; Roitberg, A. E.; Krause, J. L. *Phys. Rev. Lett.* **2004**, *92*, 158301.
- (24) Comstock, M. J.; Chi, J.; Kirakosian, A.; Crommie, M. F. *Phys. Rev. B* **2005**, *72*, 153414.
- (25) Moresco, F. Private communication.
- (26) Pascual, J. I.; Henningsen, N. Private communication.
- (27) Frisch, M. J.; Trucks, G. W.; Schlegel, H. B.; Scuseria, G. E.; Robb, M. A.; Cheeseman, J. R.; Zakrzewski, V. G.; Montgomery, J. A., Jr.; Stratmann, R. E.; Burant, J. C.; Dapprich, S.; Millam, J. M.; Daniels, A. D.; Kudin, K. N.; Strain, M. C.; Farkas, O.; Tomasi, J.; Barone, V.; Cossi, M.; Cammi, R.; Mennucci, B.; Pomelli, C.; Adamo, C.; Clifford, S.; Ochterski, J.; Petersson, G. A.; Ayala, P. Y.; Cui, Q.; Morokuma, K.; Malick, D. K.; Rabuck, A. D.; Raghavachari, K.; Foresman, J. B.; Cioslowski, J.; Ortiz, J. V.; Baboul, A. G.; Stefanov, B. B.; Liu, G.; Liashenko, A.; Piskorz, P.; Komaromi, I.; Gomperts, R.; Martin, R. L.; Fox, D. J.; Keith, T.; Al-Laham, M. A.; Peng, C. Y.; Nanayakkara, A.; Gonzalez, C.; Challacombe, M.; Gill, P. M. W.; Johnson, B.; Chen, W.; Wong, M. W.; Andres, J. L.; Gonzalez, C.; Head-Gordon, M.; Replogle, E. S.; Pople, J. A. *Gaussian 98*, revision A.7; Gaussian Inc.: Pittsburgh, PA, 1998.
- (28) Becke, A. D. *J. Chem. Phys.* **1993**, *98*, 5648.
- (29) Casida, M. E.; Jamorski, C.; Casida, K. C.; Salahub, D. R. *J. Chem. Phys.* **1998**, *108*, 4439.
- (30) McLean, A. D.; Chandler, G. S. *J. Chem. Phys.* **1980**, *72*, 5639.
- (31) Krishnan, R.; Binkley, J. S.; Seeger, R.; Pople, J. A. *J. Chem. Phys.* **1980**, *72*, 650.
- (32) Ditchfield, R.; Hehre, W. J.; Pople, J. A. *J. Chem. Phys.* **1971**, *54*, 724.
- (33) Hehre, W. J.; Ditchfield, R.; Pople, J. A. *J. Chem. Phys.* **1972**, *56*, 2257.
- (34) Hariharan, P. C.; Pople, J. A. *Theor. Chim. Acta* **1973**, *28*, 213.
- (35) Clark, T.; Chandrasekhar, J.; Spitznagel, G. W.; Schleyer, P. v. R. *J. Comput. Chem.* **1983**, *4*, 294.
- (36) Gritsenko, O. V.; Baerends, E. J. *J. Chem. Phys.* **2002**, *117*, 9154.
- (37) Henzl, J.; Mehlhorn, M.; Gawronski, H.; Rieder, K. H.; Morgenstern, K. *Angew. Chem., Int. Ed.*, in press.
- (38) Walkup, R. E.; News, D. M.; Avouris, Ph. *Phys. Rev. B* **1993**, *48*, 1858.
- (39) Gao, S.; Persson, M.; Lundquist, B. I. *Solid State Commun.* **1992**, *84*, 271.
- (40) Persson, B. N. J.; Avouris, Ph. *Surf. Sci.* **1997**, *45*, 390.
- (41) Gao, S.; Persson, M.; Lundquist, B. I. *Phys. Rev. B* **1997**, *55*, 4825.
- (42) Ma, G.; Guo, H. *Chem. Phys. Lett.* **2000**, *317*, 315.
- (43) Abe, A.; Yamashita, K.; Saalfank, P. *Phys. Rev. B* **2003**, *67*, 235411.
- (44) Saalfank, P. *J. Chem. Phys.* **2000**, *113*, 3780.
- (45) Bouwstra, J. A.; Schouten, A.; Kroon, J. *Acta Crystallogr., Sect. C* **1983**, *39*, 1121.
- (46) Mostad, A.; Rømming, C. *Acta Chem. Scand.* **1971**, *25*, 3561.
- (47) Andersson, J.-A.; Petterson, R.; Tegnér, L. *J. Photochem.* **1982**, *20*, 17.
- (48) Jaffé, H. H.; Yeh, D.-J.; Gardner, R. W. *J. Mol. Spectrosc.* **1958**, *2*, 120.